INDUCED ANISOTROPY IN A CYLINDRICAL NEODYMIUM-DOPED GARNET COMPONENT

Yu. A. Golyaev, K. N. Evtyukhov,
and L. N. Kaptsov

Vestnik Moskovskogo Universiteta. Fizika,
Vol. 35, No. 1, pp. 29-35, 1980

UDC 535.551

A calculation is performed on the induced birefringence in a cylindrical garnet rod having a parabolic temperature distribution. An estimate is made of the effects of the induced anisotropy on the lasing performance and on the gain for linearly polarized radiation in a cavity containing a component in which the birefringence varies over the cross-section. The theoretical results are compared with experiment. The effects of residual stresses have been determined.

A thermal-stress pattern is set up in an active element AE in a laser or light amplifier based on neodymium-doped garnet [1, 2] because some of the pumping energy is deposited as heat in the material and the side surface of the rod is cooled by a flowing liquid. These stresses cause anisotropy in the refractive index and an uneven distribution of birefringence over the cross-section. The rod is usually cylindrical, with the length much greater than the transverse dimensions. In that case, the condition at the mounting end has little effect on the stress distribution [2]. Also, the cooling conditions are normally uniform over the side surface. One can therefore assume that the induced birefringence is dependent only on the transverse coordinates and does not vary along the length of the AE.

Several studies [3-6] have shown that birefringence inhomogeneously distributed over the cross-section largely determines the parameters of the generated or amplified radiation. Therefore, the exact determination of the birefringence distribution is of considerable practical significance in optimizing parameters of lasers and light amplifiers.

If the AE is a cylindrical rod, the distribution of the thermally induced birefringence is dependent on the orientation of the axis of the cylinder relative to the axes of the cubic lattice in the garnet crystal. Studies have been made [1, 2, 7] on rods in which the axis coincided with the <111> crystallographic direction. In that case, the induced birefringence is dependent on the distance to the axis of the cylinder and is independent of the angular coordinates. On the other hand, rods with <001> crystallographic orientation are are widely used. A theoretical study [8] shows that then the induced birefringence is dependent on the radial and angular coordinates. Few experiments have been performed on this. Only in [9] do we find the study related to the determination of the astigmatism in the thermal lens. In all the above studies, the tensor features were considered only for the elastooptic effect, while the garnet was considered as isotropic in defining the stress pattern. The theory of elasticity for anisotropic bodies can be applied to avoid this assumption without complicating the calculation.

© 1980 by Allerton Press, Inc.

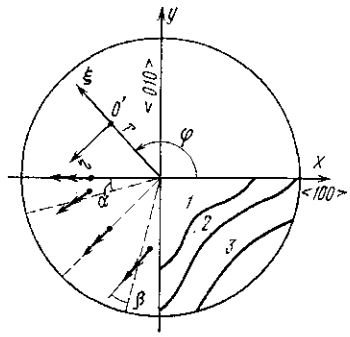

Fig. 1. Disposition of the coordinate axes (first and second quadrants) and of one of the axes of the optical indicatrix in relation to the angular coordinate (third quadrant); also line of equal phase shift (fourth quadrant); $\alpha = 14.8°$, $\beta = 15.5°$.

Here we calculate the induced birefringence in a cylindrical garnet rod of <001> orientation and estimate the effects of the birefringence on the lasing performance and the amplification of linearly polarized light; experimental results are given that indicate a substantial role for the initial stresses in the cold AE.

We consider a cylindrical rod of radius R and length L; we assume that the temperature T_0 is the same everywhere on the side surface, while the density of heat production P is constant throughout the volume of the rod. The temperature distribution is then familiar:

$$T(r) = T_0 + \frac{P}{4\varkappa}(R^2 - r^2), \tag{1}$$

where r is the distance from the axis of the cylinder and $\varkappa$ is the thermal conductivity, which is a scalar for a cubic crystal. The method of calculating the thermal stress used in the theory of elasticity for anisotropic bodies is to be found in [10]. This involves solving a system of tensor equations for the elastic equilibrium and equations for the compatibility of the strains. Here we use the results of [11], where the stresses were calculated for bodies of cylindrical form with a parabolic temperature distribution of (1).

The stress tensor σ is diagonal and has the following components in the local coordinate system $O'\xi\eta z$ (Fig. 1):

$$\begin{aligned} \sigma_{\xi\xi} &= \sigma_r = \alpha P R^2 D(\zeta - 1)(2\varkappa)^{-1}; \\ \sigma_{\eta\eta} &= \sigma_\varphi = \alpha P R^2 D(3\zeta - 1)(2\varkappa)^{-1}; \\ \sigma_{zz} &= \sigma_z = (0{,}125 - s_{12}D)\,\alpha P R^2 (2\zeta - 1)(s_{11}\varkappa)^{-1}, \end{aligned} \tag{2}$$

where $\zeta = r^2/R^2$; $D = (s_{11} - s_{12})(6s_{11}^2 - 8s_{12}^2 + 2s_{11}s_{12} + s_{11}s_{44})^{-1}$; s_{11}, s_{12}, s_{44} are the elastic-compliance constants and α is the coefficient of thermal expansion.

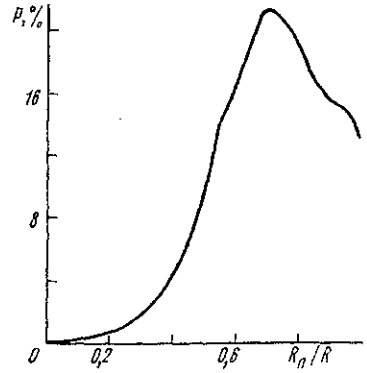

Fig. 2. Energy enhancement for linearly polarized light on optimizing the position of the rod in relation to beam radius ($\mathcal{P}$ = 100 W).

The numerical values of the stresses given by (2) are less by 30% than those calculated from the formulas in the theory of isotropic media [9], and the difference may be important if one has to determine the failure stresses at high pumping levels.

When the thermal-stress distribution is known, the usual method [2] can be used to determine the local changes in the optical indicatrix. As a result we get that the tensor for the increments in the coefficients of the optical indicatrix in the $O'\xi\eta z$ system will take the form

$$\Delta B = \begin{pmatrix} \Delta B_{rr} & \Delta B_{r\varphi} & 0 \\ \Delta B_{r\varphi} & \Delta B_{\varphi\varphi} & 0 \\ 0 & 0 & \Delta B_{zz} \end{pmatrix},$$

where the following are the components different from zero:

$$\begin{aligned} \Delta B_{rr} &= \sigma_z \pi_{12} + \frac{1}{4}\cos 4\varphi\,[(\pi_{12} + \pi_{44} - \pi_{11})(\sigma_\varphi - \sigma_r) + \\ &+ \sigma_r(3\pi_{11} + \pi_{12} + \pi_{44}) + \sigma_\varphi(3\pi_{12} + \pi_{11} - \pi_{44})]; \\ \Delta B_{\varphi\varphi} &= \sigma_z \pi_{12} + \frac{1}{4}\cos 4\varphi\,[(\pi_{12} + \pi_{44} - \pi_{11})(\sigma_r - \sigma_\varphi) + \\ &+ \sigma_r(3\pi_{12} + \pi_{11} - \pi_{44}) + \sigma_\varphi(3\pi_{11} + \pi_{12} + \pi_{44})]; \\ \Delta B_{r\varphi} &= \left(\frac{1}{4}\right)\sin 4\varphi\,(\pi_{44} + \pi_{12} - \pi_{11})(\sigma_r - \sigma_\varphi); \\ \Delta B_{zz} &= \pi_{11}\sigma_{zz} + \pi_{12}(\sigma_r + \sigma_\varphi). \end{aligned} \tag{3}$$

Compliances σ_φ, σ_r and σ_z appearing here and the piezooptic coefficients π_{ij} may be calculated from the elastic-rigidity constants and the elastooptic coefficients available from the literature [2]:

$$s_{11} = 3{,}591\cdot 10^{-12}\ \text{m}^2/\text{N};\ s_{12} = -0{,}897\cdot 10^{-12}\ \text{m}^2/\text{N};$$

$$s_{44} = 8{,}688\cdot 10^{-12}\ \text{m}^2/\text{N};\ \pi_{11} = -0{,}1205\cdot 10^{-12}\ \text{m}^2/\text{N};$$

$$\pi_{12} = 0{,}05053 \cdot 10^{-12}\ \mathrm{m^2/N};\ \pi_{44} = -0{,}5343 \cdot 10^{-12}\ \mathrm{m^2/N}.$$

It follows from (3) that a garnet crystal optically isotropic in the cold state becomes biaxial under pumping; the birefringence is determined by the lengths and positions of the semiaxes of the ellipse obtained by section of the optical indicatrix by the plane z = 0 for rays propagating along the z axis. The angle χ between the $O'\xi$ axis and the nearest semiaxis of the ellipse is found from

$$\operatorname{tg} 2\chi = \frac{2\Delta B_{r\varphi}}{\Delta B_{rr} - \Delta B_{\varphi\varphi}} = \frac{\sin 4\varphi}{\Pi_1/\Pi_2 - \cos 4\varphi}; \qquad (4)$$
$$-45^\circ \leqslant \chi \leqslant 45^\circ,$$

where $\Pi_1 = \pi_{44} + \pi_{11} - \pi_{12}$; $\Pi_2 = \pi_{44} + \pi_{12} - \pi_{11}$. The maximum deviation of the axes of the ellipse from the axes of the local coordinate system is about 15.5° for $\varphi \simeq 14{,}8^\circ + n(\pi/2)$ $(n = 0, 1, 2...)$. Figure 1 shows the approximate orientation of the axes of the ellipse in one of the quadrants. The phase difference θ between waves linearly polarized along the axes of the ellipse on passage through the entire length of the AE is given by

$$\theta = \frac{\mathcal{P} n_0^3 \alpha D \zeta}{2\lambda \varkappa} \sqrt{\Pi_1^2 + \Pi_2^2 - 2\Pi_1\Pi_2 \cos 4\varphi} =$$
$$= 2\zeta A(4\varphi), \qquad (5)$$

where $\mathcal{P} = \pi L R^2 P$ is the total thermal power dissipated throughout the AE and λ is the wavelength of the light. It follows from (5) that the sign of the birefringence is the same throughout the cross-section. We substitute the numerical values for radiation with wavelength λ = 1.06 μm into (5) to get

$$\theta(\varphi_{\max}) \cong 0{,}101\,(r^2/R^2)\,\mathcal{P}\ \ \mathrm{rad/W};$$
$$\theta(\varphi_{\min}) \cong 0{,}032\,(r^2/R^2)\,\mathcal{P}\ \ \mathrm{rad/W}; \qquad (6)$$

where $\varphi_{\max} = \pi/4 + k\pi/2$; $\varphi_{\min} = k\pi/2$ $(k = 0, 1, 2, 3)$. It is found [1] that the thermal power dissipated in a neodymium-doped garnet rod may be 5-7% of the electrical power supplied to the pumping lamp. It then follows from (6) for pumping powers of 2-3 kW typical of continuous-wave lasers that the phase difference at the edge of the rod may be several radians. As an example, Fig. 1 shows the lines of equal phase difference $\theta = \pi/2, \pi, 2\pi$ in the fourth quadrant for light of wavelength λ = 1.06 μm for a thermal power $\mathcal{P} = 100$ W.

We now estimate one of the possible effects from the inhomogeneous birefringence on the lasing or amplification. In many cases, the rod in the generator or amplifier is combined with a polarizer in order to obtain linearly polarized radiation. We now estimate what fraction of the energy in a beam of linearly polarized light passing through such a rod described by (4) and (5) is transferred to the wave polarized perpendicular to the initial one and absorbed or deflected from the beam by the polaroid. The intensity of the wave incident on the rod is assumed to be constant over the cross-section of the beam of radius $R_b \leqslant R$. The plane of polarization of the incident light (the plane of transmission of the polarizer) lies at an angle γ to the <001> direction. Then the following is the power in the wave polarized perpendicular to the initial one when the beam has passed through the rod:

$$W_{\perp} = I_0 \int_0^{2\pi} \int_0^{R_b} \sin^2 2[\varphi + \chi(\varphi) - \gamma] \sin^2\left(\frac{\theta}{2}\right) r dr d\varphi =$$

$$= \frac{R_b^2 I_0}{8} [a(\zeta) + b(\zeta) \cos 4\gamma],$$

where $\xi = (R_b/R)^2$, R_b is the beam radius, and I_0 is the intensity in the incident beam:

$$a(\zeta) = 2\pi - \int_0^{\pi} \sin[2\zeta A(\psi)] \cdot [\zeta A(\psi)]^{-1} d\psi;$$

$$b(\zeta) = \int_0^{\pi} \cos[\varphi + \chi(\varphi)] \left\{ \frac{\sin 2\zeta A(\psi)}{\zeta A(\psi)} - 2 \right\} d\psi.$$

While the beam passes through the rod once in a ring laser or in a one-part amplifier, it passes through twice in a linear laser, which is equivalent to doubling the thermal power. The relative losses $\delta = W_{\perp}/W_0 = [a(\zeta) + b(\zeta) \cos 4\gamma]/8\pi$ are maximal when the plane of transmission of the polarizer coincides with the <100> or <010> direction, i.e., for $\varphi = k\pi/2$, and are minimal for $\varphi = \pi/4 + k\pi/2$. The enhancement of the energy in the polarized light when the polarizer is correctly disposed can be characterized by $p = \left(\frac{1-\delta_{min}}{1-\delta_{max}} - 1\right) \cdot 100\%$. Figure 2 shows the dependence of p on R_b/R for λ = 1.06 μm. Maximum loss occurs for $R_b/R \simeq 0{,}7$ and constitutes 22%. The enhancement of the power of the linearly polarized light for $R_b/R >$ > 0.5 is 15-20%. In the generation or amplification of the fundamental transverse wave, which has a gaussian intensity distribution over the cross section, the strong birefringence at the edge of the rod will have substantially less effect on the production of linearly polarized light.

The birefringence parameters were measured on several rods differing in size, optical quality, and form of lamp house. The pumping was approximately uniformly distributed over the cross-section. The positions of the axes of the indicatrix were determined by photography of the conoscopic figures. A rod mounted in the lamp house was placed between two crossed polaroids, which rotated together around the axis, and through which a beam of red light from a helium-neon laser was passed. The directions of the ends of the dark cross (the isogyres) defined the angular coordinates of the points at which one of the axes of the indicatrix is parallel to the plane of transmission of the first polaroid. The phase differences θ for the various parts of the rod were determined by means of a narrow (diameter about 0.5 mm) beam of plane-polarized light from an He-Ne laser (λ = = 0.63 μm) or from continuous-wave neodymium-garnet laser (λ = 1.06 μm). The ellipticity of the light emerging from the rod was used to calculate θ. Figure 3 shows typical conoscopic figures for two rods. Specimen 1 was of larger volume than specimen 2 and was inserted in the light house with a more efficient reflector. The birefringence in specimen 1 was the larger, as was evident from the occurrence of isochromic lines with phase difference of 360° when the pumping exceeded 1.5 kW. The conoscopic figures for several specimens showed that there was always appreciable anisotropy even in the cold state. Figure 4 shows the theoretical relationship between the positions of the axes of the indicatrix Φ and the angle φ, together with the corresponding measurements for specimens 1 and 2 at various pumping levels, as well as for specimen 1 in the cold state. The $\Phi = \Phi(\varphi)$ relation for the unpumped rod follows the form of the curve calculated for a parabolic temperature distribution. This was confirmed in measurements on

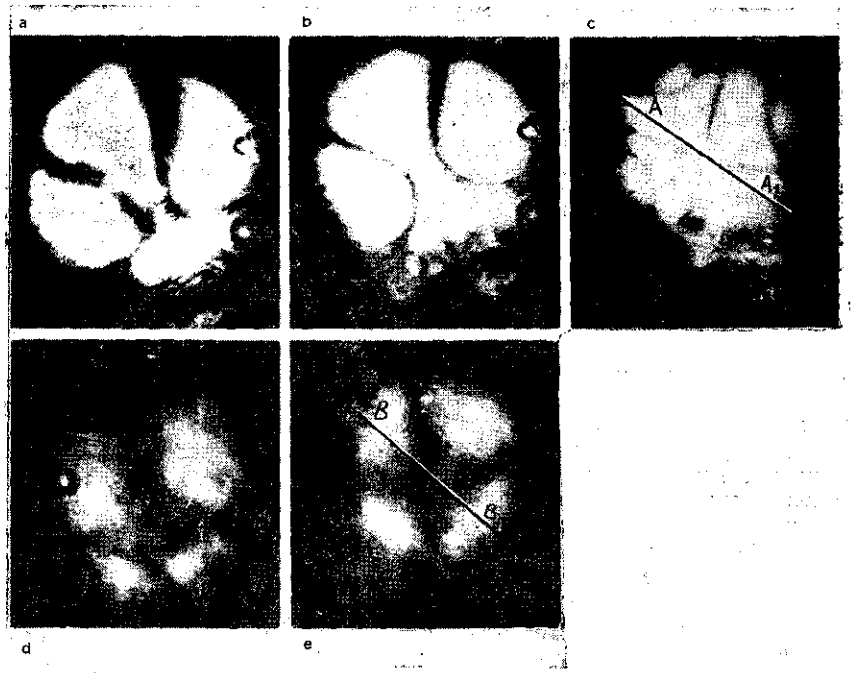

Fig. 3. Conoscopic figures for two rods. Specimen 1: without pumping (a); electrical power input to pumping lamp 1 kW (b); 2 kW (c); specimen 2: unpumped (d), and with 2 kW pumping (e).

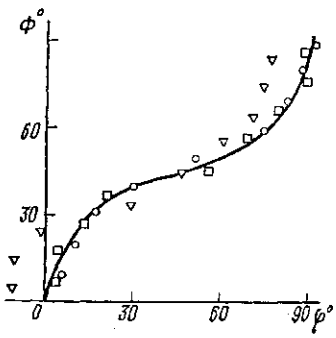

Fig. 4

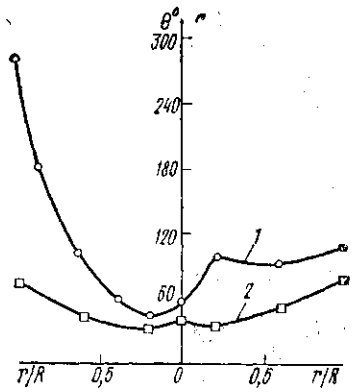

Fig. 5

Fig. 4. Rotation of the axis of the indicatrix with respect to the <100> direction in relation to the angular coordinate φ. Solid line from theory, ▽ specimen 1 without pumping, ○ and □ specimens 1 and 2 respectively pumped at 2 kW.

Fig. 5. Variation in phase difference θ over the cross section of a rod for λ = 1.06 μm: 1) specimen 1; 2) specimen 2; pumping 2 kW.

other specimens. The effect appears to be due to residual stresses arising during the growth and annealing of the rod. Birefringence distribution in the pumped rod persists in the cold state, so it was possible to orient the rod in the desired position without switching on the pumping, namely from the conoscopic figures given by the He-Ne laser.

Figure 5 gives measured phase patterns for the same specimens obtained on displacing the probe beam along the lines AA and BB in Fig. 3 at equal pumping levels. The asymmetry in the stresses in cold specimen 1 makes itself felt when the pumping is switched on, whereas specimen 2, which has lower and symmetrical initial stresses, gives parabolic distribution of the phase shift in the heated state, as the theory would imply. Such measurements allow one to determine the coefficient for the conversion of the electrical power supplied to the pumping lamp to heat in the rod. In the present case this was 2% for specimen 1 but 0.6% for specimen 2. Measurements of this kind with several rods showed that the conversion factor is only slightly dependent on the volume. For example, volume reduction by a factor 2 reduces the coefficient from 0.6 to 0.55%.

We have therefore derived and verified formulas that describe the thermally induced birefringence in a cross section of a rod of <001> orientation. An estimate has also been made of the depolarizing effect of such a rod in the generation of linearly polarized light. The distribution of the initial stresses in a cold rod resembles that in a hot rod, which provides a way of determining the optimum orientation of the rod in the cavity.

REFERENCES

1. W. Koechner, Appl. Opt. vol. 9, p. 1429, 1970.
2. J. D. Foster and L. M. Osterink, J. Appl. Phys., vol. 41, p. 3656, 1970.
3. F. M. Quelle, Appl. Opt., vol. 5, p. 621, 1966.
4. A. A. Mak, V. M. Mit'kin and L. N. Soms, Opt. i Spekt., vol. 33, p. 996, 1972.
5. P. G. Konvisar, S. R. Rustamov and A. A. Fomichev, Kvant. Elektronika, no. 1, p. 667, 1974.
6. V. G. Mikhalevich and G. P. Shipulo, Kvant. Elektronika, no. 1, p. 207, 1974.
7. W. Koechner, Appl. Opt., vol. 9, p. 2548, 1970.
8. W. Koechner and D. K. Rice, J. Opt. Soc. Amer., vol. 61, p. 758, 1971.
9. V. G. Dmitriev, B. M. Umanskii and N. V. Shkunov, Kvant. Elektronika, no. 2, p. 80, 1971.
10. Yu. I. Sirotin and M. P. Shaskol'skaya, Principles of Crystal Physics [in Russian], Moscow, 1975.
11. Yu. I. Sirotin, Kristallografiya, vol. 1, p. 708, 1956.

5 April 1978